Experimental study on thermal runaway risk of 18650 lithium ion battery under side-heating condition

Experimental study on thermal runaway risk of 18650 lithium ion battery under side-heating condition

Huang Li[a], Haodong Chen[a], Guobin Zhong[b], Yu Wang[c], Qingsong Wang[a,*]

Email： *pinew@ustc.edu.cn*

[a] State Key Laboratory of Fire Science, University of Science and Technology of China, Hefei 230026, China

[b] Electric Power Research Institute of Guangdong Power Grid Co. Ltd., Guangzhou 510080, Guangdong, China

[c] BRE Centre for Fire Safety Engineering, University of Edinburgh, Edinburgh EH9 3JL, United Kingdom

Abstract

To simulate the heat transfer between lithium-ion batteries (LIBs), an electric heater with the same size and shape as the LIB is used to trigger thermal runaway event in this work. The effect of state of charge (SOC), the power of the heater, the spacing on thermal behavior of LIB was investigated as well the amount of transferred heat between the heater and LIB was calculated. The results indicate that 50% SOC is an unstable state for LIB, that a stronger jet flame becomes more likely when the SOC of LIB is higher than 50%. Additionally, the increased spacing, lower heating power and SOC can contribute to mitigate the severity of thermal runaway behavior. Further, the dominant path of heat transfer between the heater and LIB will also vary with operating conditions. The heat conduction through air is the main heat transfer path in tests with lower heating power. However, heat radiation will replace heat conduction as the primary heat transfer mode when there is a large temperature difference between the heater and LIB in tests with higher heating power. Understanding the leading heat transfer path between LIBs can provide valuable guidelines for the safety design of lithium-ion battery modules.

Key words: *lithium ion battery safety, thermal runaway, side-heating, state of charge, electric heater*

1. Introduction

Due to the high density and long cycle life, the lithium-ion battery (LIB) has be-

* Corresponding authors: Q.S. Wang: Tel.: +86 551 6360 6455; fax: +86 551 6360 1669. E-mail: pinew@ustc.edu.cn;

come a promising choice for powering electric vehicles in recent years. However, the fire and explosion accidents related to the thermal runaway event of LIBs were reported from time to time (Lisbona & Snee, 2011). Further, these accidents prompted global attention to the potential fire risks of lithium-ion battery in practical applications.

Thermal runaway behavior of the single cell under special abnormal conditions had been extensively studied (Jhu et al., 2011; Larsson & Mellander, 2014; Peng et al., 2014; Fu et al., 2015). As the temperature builds up, the solid electrolyte interphase (SEI) layer will start to decompose at 90-120 ºC (Wang et al., 2012). Then, the reaction of intercalated lithium with electrolyte, the decomposition reactions of electrolyte, negative and positive active material will be initiated sequentially with the increasing temperature (Wang et al., 2006; Wu et al., 2018). In addition, the heat generated by these chemical exothermic reactions from the cells will further accelerate these reactions and release more heat. Lastly, the thermal runaway event will be triggered once the temperature value exceeds a certain threshold (Spotnitz & Franklin, 2003). Jhu et al. (Jhu et al., 2012) have investigated the thermal runaway potential of the 18650 LIB with different cathodes using an adiabatic calorimeter, the peak temperature of the LIB with 100% SOC in thermal runaway could reach to 665-709 ºC. Liu et al. (Liu et al., 2015) have conducted tests to measure the generated heat energy inside the 2.2 Ah LIB through Copper Slug Battery Calorimetry (CSBC). The results showed that the value of the generated energy increased with increasing state of charge, that the peak value is 34.0 ± 1.8 kJ. Furthermore, Wang et al (Wang et al., 2017) have studied the combustion behavior of the 50 Ah LiFePO4/graphite battery through the ISO 9705 combustion room, the present results indicate that the maximum heat release rate could reach 64.32 kW and the maximum heat release was 13.74 MJ.

However, a large amount of LIBs are always connected to form the module in practical applications in order to satisfy the demands of power. Thus, if a single cell in the module undergoes thermal runaway, the released heat can expose the other LIBs to a high temperature environment and even cause the whole battery module get into thermal runaway. Lopez et al. (Lopez et al., 2015) have experimental studied thermal runaway and propagation behavior in lithium-ion battery module, and the results indicated that the increased spacing and appropriate connected tab style both contribute to the prevention of thermal runaway propagation event. Feng et al. (Feng et al., 2015; Feng et al., 2015) carried out thermal runaway propagation experiments within lithium-ion battery modules that formed by six LIBs, they revealed the thermal runaway propagation mechanism between LIBs. Lamb et al. (Lamb et al., 2015) had conducted thermal runaway propagation tests in LIB modules with different electric connection styles, and also present the temperature and voltage variations in the experiments (Lamb et al., 2015). During these cases, the released intense heat from a single cell in thermal runaway will violently heat its neighbors in one side and lead to the significant temperature rise of neighbor LIBs. The adjacent LIBs are heated unevenly and the significant temperature difference will be formed on the surfaces of the LIBs.

However, the thermal runaway propagation test is hard to conduct as the complex circuit connection and a large amount of measuring points. In addition, these tests also have the high fire or even explosive risks as the violent jet flame and a considerable amount of combustible and toxic gases (Nedjalkov et al., 2016; Sun et al., 2016; Larsson et al., 2018).

In this work, a heater was used to trigger the thermal runaway of the LIB. In order to simulate the heat transfer process between a LIB in thermal runaway and its adjacent LIB, the size and shape of the heater is designed to be the same as sample cells. Furthermore, the maximum temperature of the 200 W heater is close to the peak temperature of the LIB in thermal runaway (Zhong et al., 2018). The LIBs in this work will be heated by the heaters which are placed on one side of lithium-ion battery. Therefore, the heater used in this work can be assumed as a lithium-ion battery in thermal runaway. The triggered mode in this work significant reduces the operational complexity and experimental risks. Besides, the effect of SOC, the power of heater and the cell spacing on thermal runaway behavior of the LIB were investigated. The calculated value of the transferred heat between the heater and LIB in this work is a valuable variable, which can contribute to analyze the dominated path of heat transfer between the heater and LIB.

2. Experimental

The representative 18650 lithium-ion batteries with $Li(Ni_xCo_yMn_z)O_2$ cathode were selected as the samples to investigate the thermal behavior in side-heating tests. In lithium-ion battery module, the intense heat from the cell in thermal runaway can result in the significant temperature rise of its neighbors. For the purpose of investigation, the power of the heater was cut off immediately as soon as the safety venting of the LIBs. Similar to the situation in lithium-ion battery module, the LIB in this work was heated in one side by the cylindrical electric heater with different powers.

The arrangement of the devices and the location of the thermocouples are shown in Fig. 1. Four 1 mm K-type chromel–alumel thermocouples (T_0-T_3) with 1 s response time and ±1.0 °C accuracy were used to measure the temperature variations of the heater and LIB. Three thermocouples (T_1-T_3) were fixed on surfaces of the cell, in which T_2 and T_3 are the recorded temperature variations of sidewalls of LIB. Because of the symmetry of the battery and the position of the thermocouple, $T_{2\text{-}3}$ (the average value of T_2 and T_3) are used to represent temperature variation of the sidewall. Further, T_1 was mounted on the surface of the LIB that far from the heater. Besides, T_0 is the thermocouple which was used to measure the temperature of the heater.

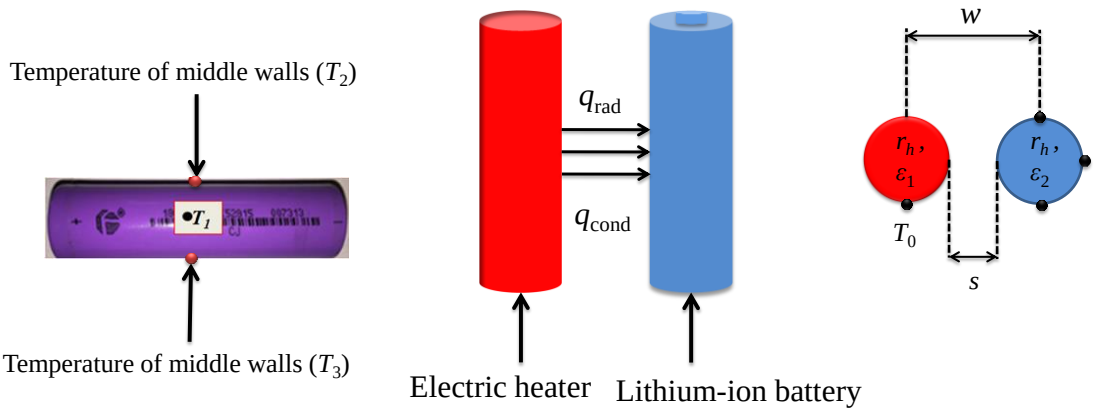

Fig. 1. The arrangement of the devices and the location of thermocouples.

Fig. 2 shows the experimental devices to record the thermal responses for LIB. In order to protect the devices and people from the sputtering materials, these experiments were conducted in a battery safety control cabinet. The size of the safety control cabinet is 1.32 × 1.0 × 2.2 m, in which was equipped with the safety observation windows to monitor the thermal runaway behavior of lithium-ion battery.

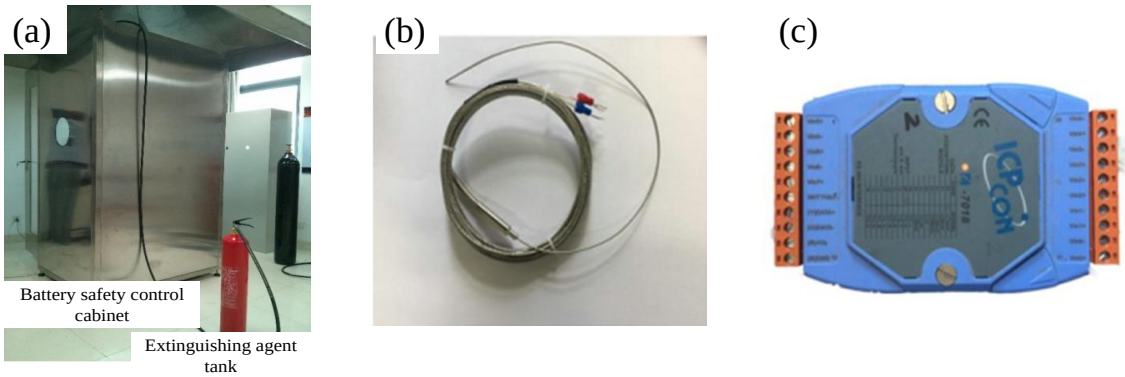

Fig. 2. Schematic of the experimental devices; a) photo of the battery safety control cabinet; b) photo of the K-type thermocouple; c) photo of the temperature logger module.

The LIB was heated to safety venting in this work, and then the power of the heater was cut off immediately. The thermal behavior of the LIB in these tests was monitored by a digital camera. The effect of SOC, the power of the heater and the cell spacing on thermal runaway behavior were investigated, respectively. As shown in Table 1, the cells with various SOCs (0%, 20%, 40%, 50%, 60%, 80%, 100%) were heated by a 200 W heater without spacing in Tests 1-7, respectively. Moreover, the cells with various SOCs were heated with 2 mm spacing in Tests 8-13. Further, the heating power was 400 W in Tests 11-16, but the spacing in Tests 11-13 and 14-16 was 2 mm and 5 mm, respectively.

Table 1 Experimental conditions of side-heating tests.

No.	Spacing / mm	SOC	The power of the heater / W
1		0%	
2		20%	
3		40%	
4	0	50%	200
5		60%	
6		80%	
7		100%	
8		0%	
9	2	50%	200
10		100%	
11		0%	
12	2	50%	400
13		100%	
14		0%	
15	5	50%	400
16		100%	

3. Results and discussion

3.1 The thermal response of the lithium-ion batteries with various SOCs

The thermal responses of the lithium-ion batetry during these experiments can be roughly divided into three stages. Fig. 3 shows the representative temperature and temperature rate responses for the LIB with 100% SOC in Test 7. In stage I，the temperature of the LIB was increased constantly by the heater, and a significant temperature difference between T_1 and $T_{2\text{-}3}$ was observed. At around 119 s, the LIB vented and released some hot gases when T_1 was 140 ^{o}C and $T_{2\text{-}3}$ was 159 ^{o}C, that resulting in the slight decreased of temperature rise rate. And then the LIB got into the "smolding period" in stage II, that no smoke was observed. However, the temperature of the LIB increased constantly in this stage due to the generated heat from exothermic reactions inside the LIB. Approximately at 150 s, the LIB underwent thermal runaway in stage III at 209-228 ^{o}C. Further, the temperature value quickly peaked at 626-673 ^{o}C at 155 s.

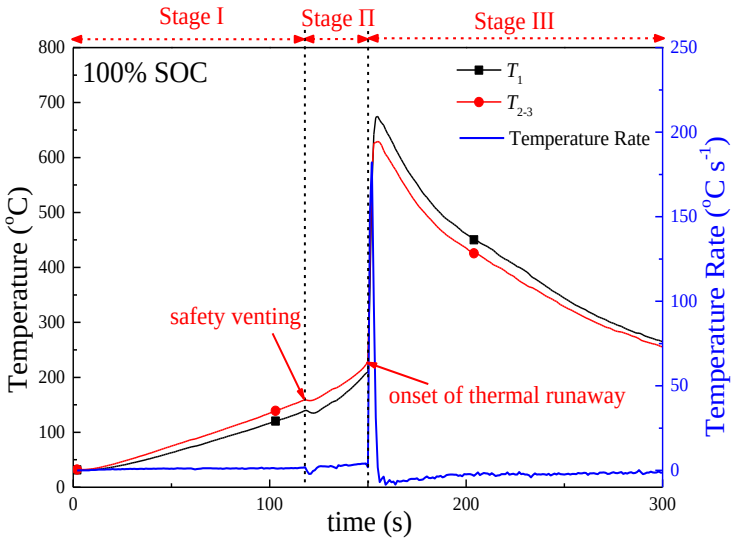

Fig. 3. The measured temperature and temperature rate responses for the LIB with 100% SOC in Test 7 without spacing.

Fig. 4 delineate the temperature and temperature rate variation profiles as a function of time for the cell with various SOCs in Tests 1-6. The results confirm that the increased SOC can significantly exacerbate thermal runaway behavior, which is manifested by the increased value of peak temperature and temperature rise rate values.

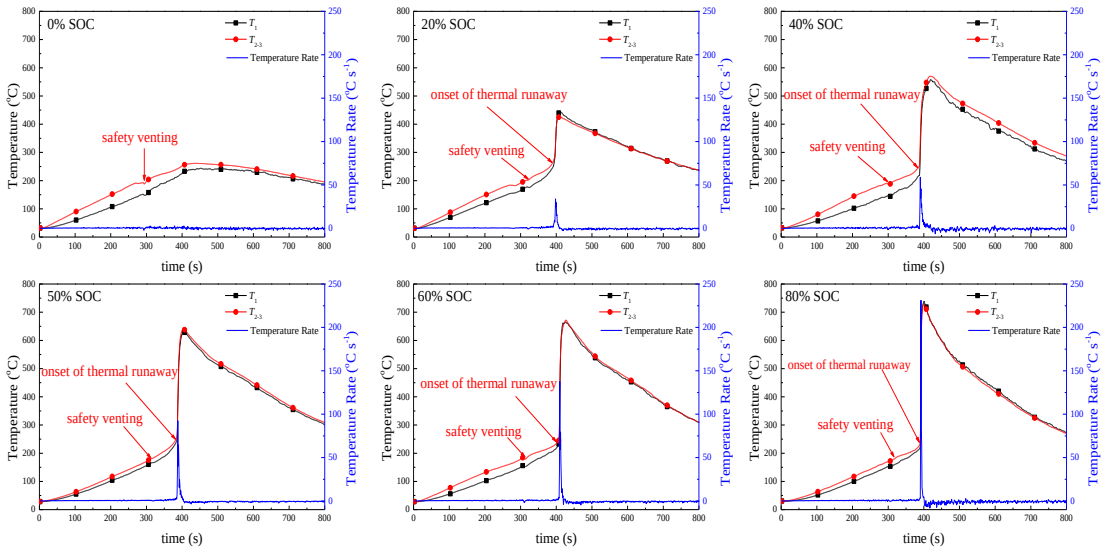

Fig. 4. The temperature and temperature rise rate in Tests 1-6 with the 200 W heater and various SOCs.

Based on these studies, the venting (T_v) and maximum temperature (T_{max}) are summarized as shown in Table 2. The results indicate that venting and maximum temperature are both determined by SOC of the LIB, and the relationships are shown in Fig. 5. It can be seen that the maximum temperature of the LIB in thermal runaway increased linearly with the increasing SOC. The higher SOC means that more electric

energy was stored in the cell. And the large scale inner short circuit will be induced when the separator is melt inside the LIB, then the electric energy could be released at a short time and contributes to the increased of temperature. In previous studies, the thermal stability of the separator inside the sample LIB was investigated using C80 calorimeter under adiabatic environment (Wu et al., 2018). The separator started to melt at 119.5 ºC and collapsed at 138.0 ºC.

Further, the increased SOC also could slightly decrease the value of venting temperature. As the temperature builds up, the exothermic reactions inside the LIB will be induced sequently. Especially, the intercalated lithium will directly react with the electrolyte solvent when the negative material loses the protection of the SEI layer and releases some combustible gases (Biensan et al., 1999; Lopez et al., 2015). Thus, the negative electrode of a LIB with higher SOC has more intercalated lithium, which will generated more gases and quickly cause the safety venting.

Table 2 Venting (T_v) and maximum temperature (T_{max}) of the LIB in Tests 1-7 with various SOCs.

Test No.	SOC	T_v	T_{max}
1	0%	193	258
2	20%	202	442
3	40%	191	570
4	50%	180	641
5	60%	186	672
6	80%	183	739
7	100%	159	673

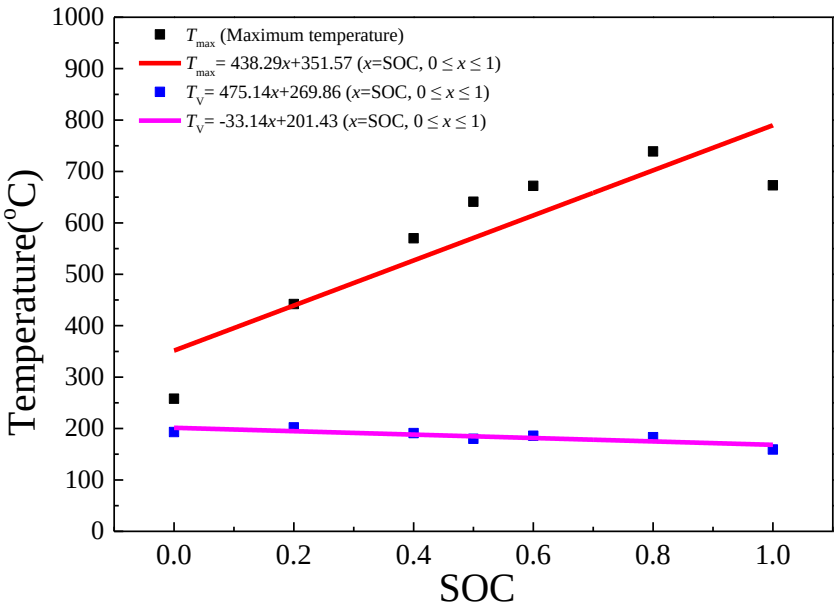

Fig. 5. Fitting curve of the maximum and venting temperature during thermal runaway as a function of SOC.

From the observed thermal behavior in these tests, the 50% SOC is an unstable state for the LIB under abuse conditions. As shown in Fig.6 (a), the LIB with lower SOC (50% or less) would experience several typical events as follows:(1) the cell was heated until safety venting and released some gases; (2) the cell entered "smoldering period" and release some gases at a lower rate; (3) the cell got into thermal runaway without jet flame and generated a considerable amount of smoke; (4) the cell is cooled to surrounding temperature. However, the LIB with a higher SOC (above 50%) in thermal runaway shows violent jet flame behavior as shown in Fig.6 (b). Besides, the effect of SOC on thermal runaway behavior is shown in Fig. 7. The mechanism of this difference may relate to the maximum temperature value of the cell and the decomposition rate of the cathode material. The decompostion reaction of cathode will release some oxygen (Kong et al., 2005), which could mix with the electrolyte solvents and then be ignited as the maximum temperature exceeds the threshold. For the LIB with lower SOC, the amounts of oxygen and generated combustible gases as well the maximum temperature may not enough to induce the jet flame.

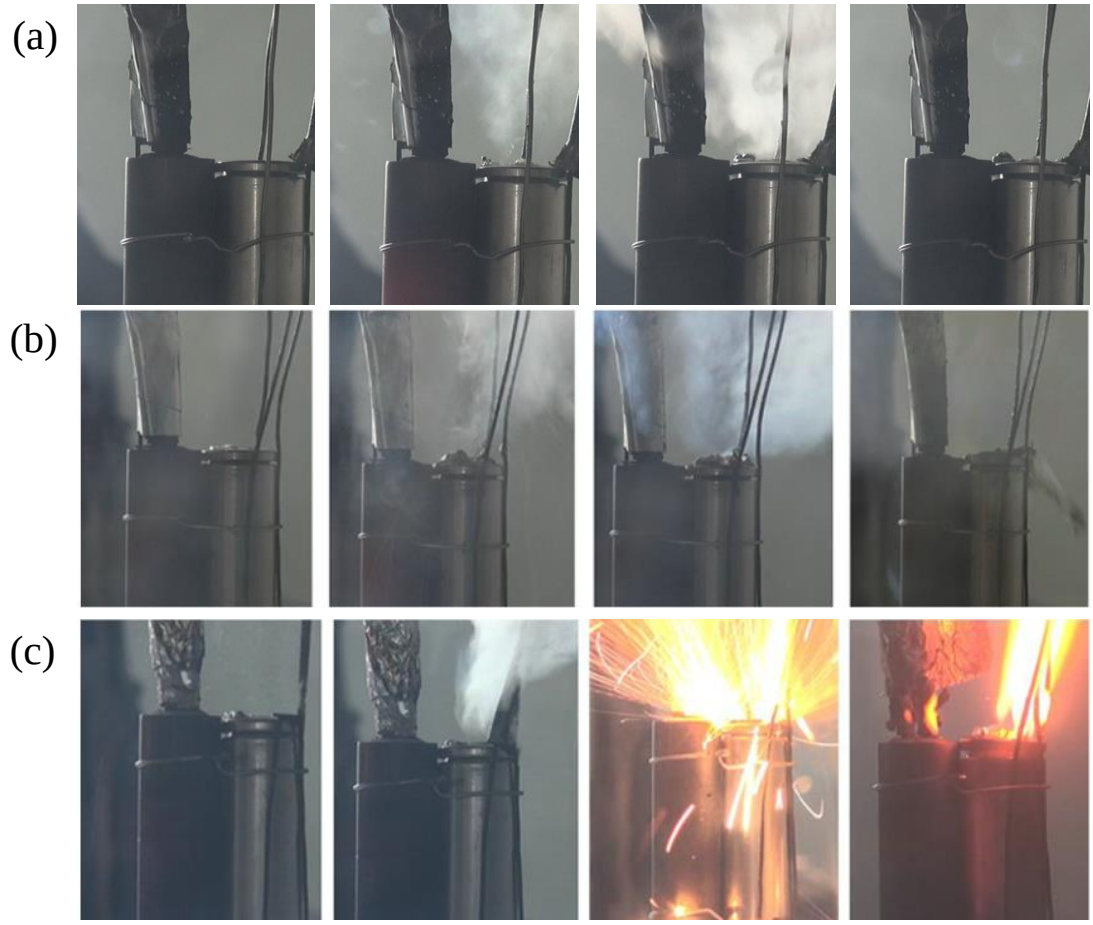

Fig. 6. The development of thermal runaway behavior in Test 1, 4 and 7; (a) photos of thermal runaway development of LIB with 0% SOC in Test 1; (b) photos of the thermal runaway development of LIB with 50% SOC in Test 4; (c) photos of the thermal runaway development of LIB with 100% SOC in Test 7.

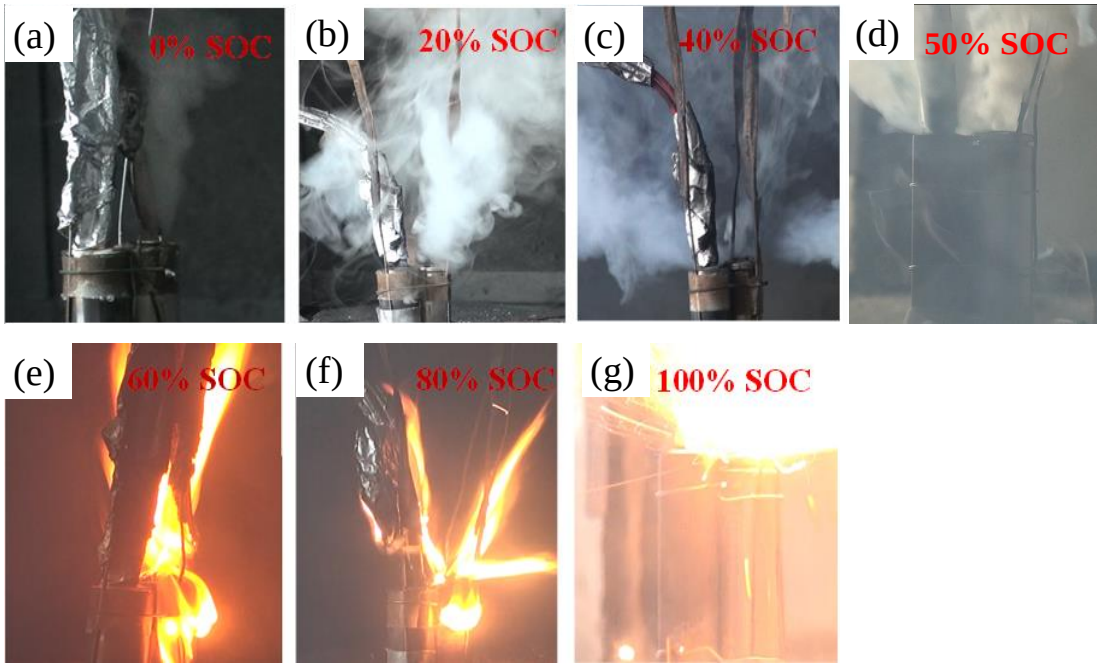

Fig. 7. The thermal runaway behaviors in Tests 1-7 with various SOCs.

3.2 The thermal response of LIBs under various heating power

In many battery modules, the certain spacing is also kept to prevent thermal runaway propagation between cells. When the heater starts to work in this work, the heat is transferred from the heater to LIB mainly by the radiation and the conduction through the surrounding air (Bergman et al., 2011; Lopez et al., 2015). For the system of two cylinders as shown in Fig. 1, the heat conduction through surrounding air can be accounted by a shape factor (Bergman et al., 2011).

$$Q = \int_0^t q(t)dt \tag{5}$$

$$q_{cond} = Sk_{air}(T_{heater} - T_{battery}) \tag{6}$$

$$S = \frac{2\pi L}{\cosh^{-1}\left(\frac{4w^2 - d_1^2 - d_2^2}{2d_1 d_2}\right)} \tag{7}$$

where S is the shape factor, k_{air} is the air thermal conductivity, L is length of the battery, w is the spacing between the center axis of heater and adjacent battery, d_1 is the diameter of heater and d_2 is the diameter of battery.

Besides, the heat radiation has much contribution to the increased temperature of the lithium-ion battery. For the cylindrical heater and sample cell, the amount of radiation heat could be considered as (Bergman et al., 2011)

$$q_{rad} = \frac{\sigma \cdot (T_{heater}^4 - T_{cell}^4)}{\frac{1-\varepsilon_1}{\varepsilon_1 A_1} + + \frac{1}{A_1 F_{12}} + \frac{1-\varepsilon_2}{\varepsilon_2 A_2}} \tag{8}$$

$$F_{12} = \frac{1}{2\pi}\left\{\pi + \left[\begin{array}{l}\left[C^2 - (R+1)^2\right]^{1/2} - \left[C^2 - (R-1)^2\right]^{1/2} \\ +(R-1)\cos^{-1}\left(\frac{R}{C} - \frac{1}{C}\right) - (R+1)\cos^{-1}\left(\frac{R}{C} + \frac{1}{C}\right)\end{array}\right]\right\} \tag{9}$$

$$R = \frac{r_h}{r_b}, R'' = \frac{s}{r_h} \tag{10}$$

$$C = 1 + R + R'' \tag{11}$$

where q_{rad} is the heat transfer rate via radiation, σ is the Stefan-Boltzmann constant, ε_1 and ε_2 is the emissivity of the heater and battery, respectively, A_1 and A_2 is the surface

area of the heater and battery, respectively. r_h and r_b are the radius for the heater and lithium-ion battery, respectively, F_{12} is the view factor of two cylinders and s is the distance between heater and the battery.

The LIB in Tests 8-10 vented at 136-150 ºC as show in Fig. 8, and then the temperature of the LIB started to decrease as the power of the heater was cut off immediately. Further, the thermal runaway event was not observed after the safety venting in Tests 8-10 with 200 W heater. It can be seen that the increased power of the heater can heat LIB more violently in Tests 11-13 with 400 W heater, and then cause the steep temperature rise of LIB. Thus, the venting temperatures of Tests 9-11 are relatively high, around 330-360 ºC. Then, the generated heat rate of the LIB exceeds its heat dissipation rate to surroundings as the high surface temperature of the heater and the LIB. And the LIBs in Tests 9 and 10 had undergone thermal runaway though the power of the heater was cut off.

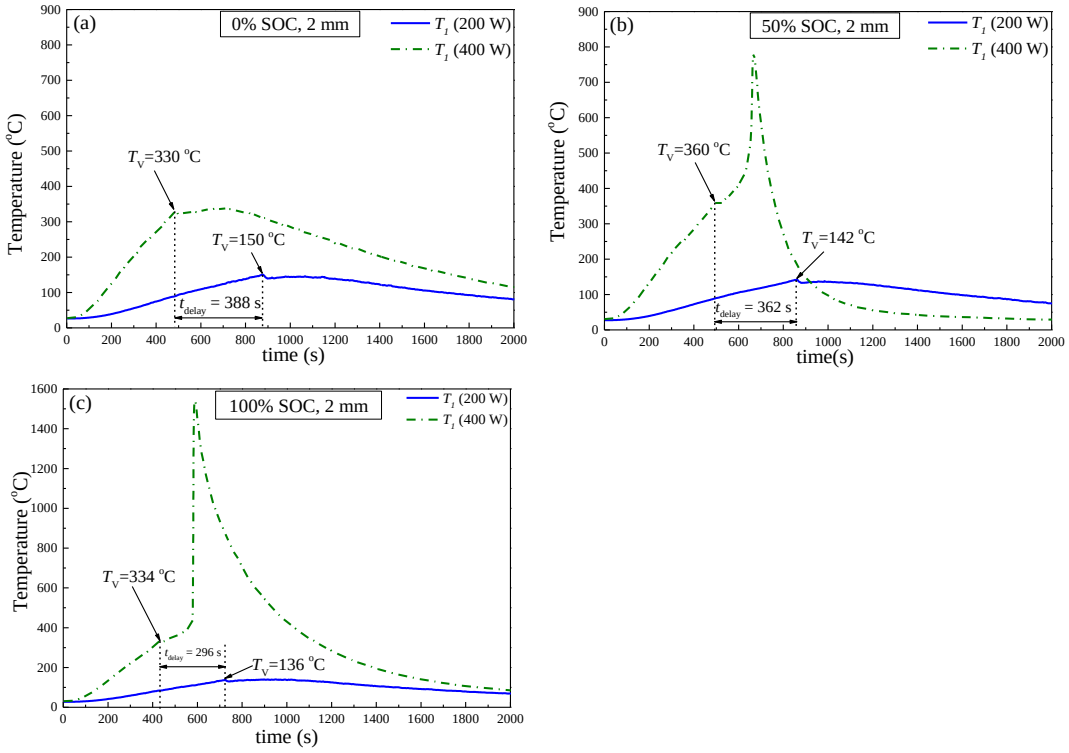

Fig. 8. The temperature response for the tests with various SOCs that the LIB are heated at 2mm spacing by 200 W and 400 W heaters, respectively.

It makes sense to understand the main heat transfer path between heater and the LIB, which can contribute to the safety design for the battery module. In Tests 8-16, the amount of heat transfer between heater and LIB from the beginning of the experiment to safety venting is calculated according to Eq. (5)-(11) as shown in Fig. 9. In Tests 8-10, the heat conduction through the surrounding air is the primary heat transfer path while the amount of radiation heat accounts for about 11.7-12.3% of the total transferred heat. And this ratio is around 56.1-61.0% in Tests 11-13. The result indicates that the heating power shows great effect on radiation heat, as well the total

amounts of the conduction and radiation heat in Tests 11-13 is also larger than the value in Tests 8-10.

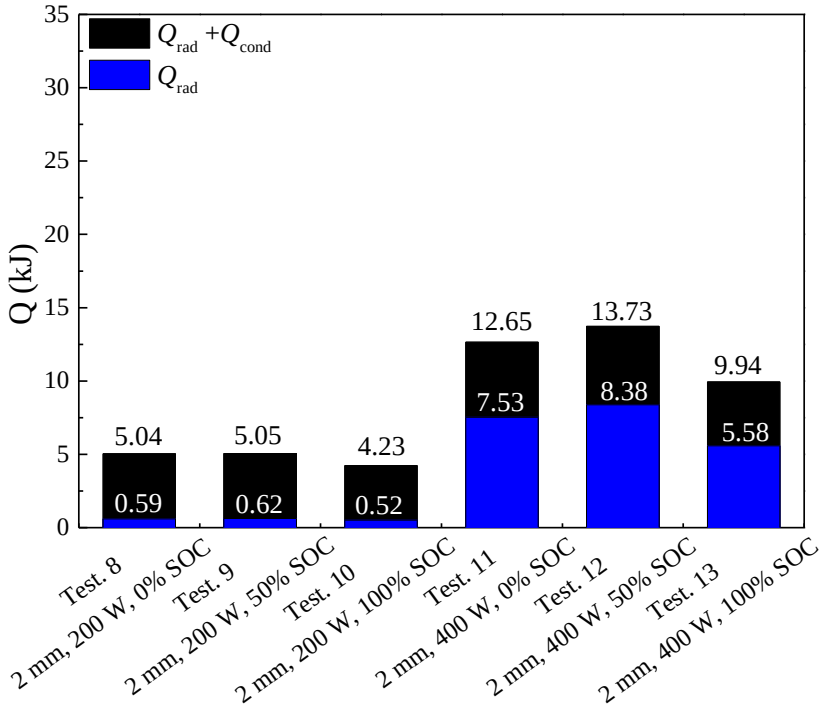

Fig. 9. The radiation and conduction heat in Tests 8-13 with with various SOCs (0%, 50%, 100%), and the cells are heated by 200 W heater in Tests 8-10 while 400 W heater in Tests 11-13.

3.3 The thermal response of LIBs with various spacing

The LIBs in Tests 8-10 were heated at 2 mm spacing and the temperature responses were compared with the results in Tests 1-7 that the spacing was 0 mm. Taking into account the differences in thermal runaway behavior, the LIBs with various SOCs (0%, 50%，100%) were selected as the samples to investigate the impact of the spacing on thermal runaway behavior, respectively. The results of the tests with 200 W heater are shown in Fig. 10. The result indicates that the increased cell spacing has a great mitigation effect on its thermal behavior. The cell spacing is kept at 2 mm in Tests 8-10, and the thermal runaway event was not initiated. Moreover, the venting time was also delayed significantly in Tests 8-10, which was approximately 400-584 s. Besides, Eq. (5)-(11) indicate that the rate of the heat transfer could decrease significantly with increasing spacing between heater and LIB. This will certainly result in a significant delay in the rupture time of the safety valve. Besides, the increased spacing could also contribute to the heat dissipation of the LIB. Thus, the temperature of the LIB will starts to decrease when the heat dissipation rate exceeds its self-heating rate and the external heating rate. And the thermal runaway event can be avoided although the LIB was vented.

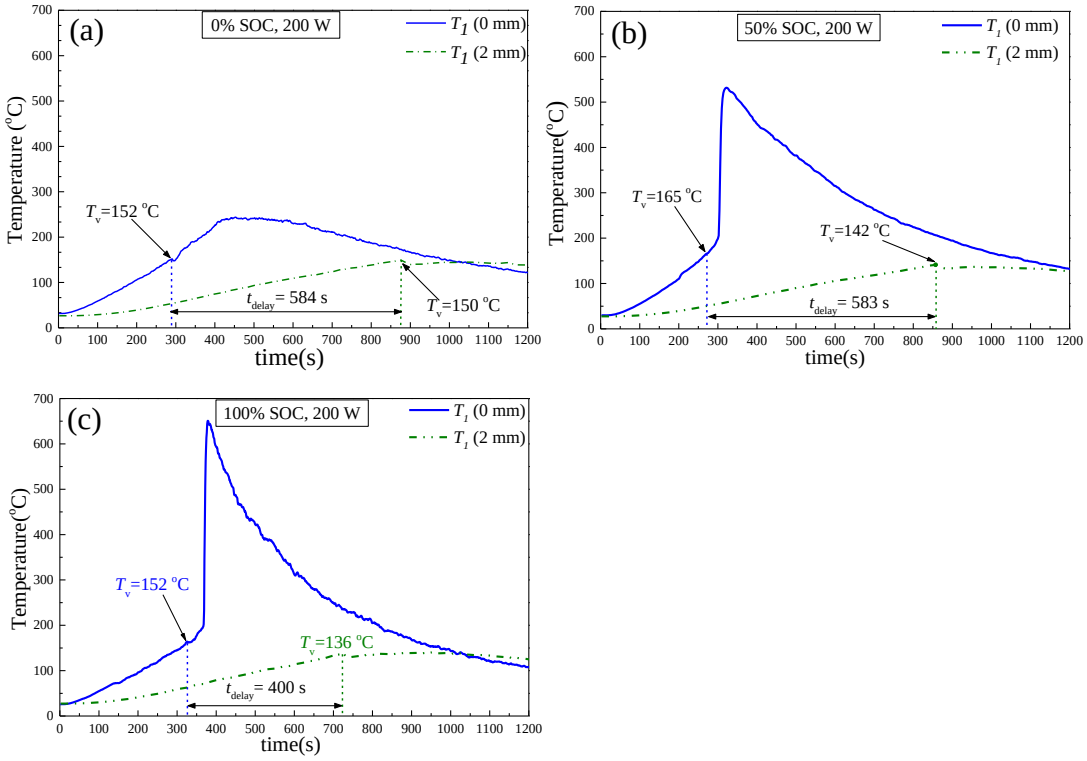

Fig. 10. The temperature response for the tests with different SOCs that the cell are heated by 200 W heater at 0 mm and 2mm spacing, respectively.

The LIBs with various SOCs were heated by 400 W heater in Tests 11-16, in which the spacing in Tests 11-13 and 14-16 is 2 mm and 5 mm, respectively. The temperature responses in Tests 11-16 are shown in Fig. 11, the venting temperature was approximately 322-376 ºC, which is much higher than that of tests with 200 W heater. Because the 400 W heater could heat the LIB violently, which results in the phenomenon that the inner temperature is still low despite the high surface temperature of the LIB. The LIB undergone thermal runaway after the safety venting in Tests 12 and 13 as the spacing was kept at 2 mm. Further, the thermal runaway event was not triggerred when the spacing was increased to 5 mm. Besides, the venting time was also delayed around 334-669 s due to the increased spacing.

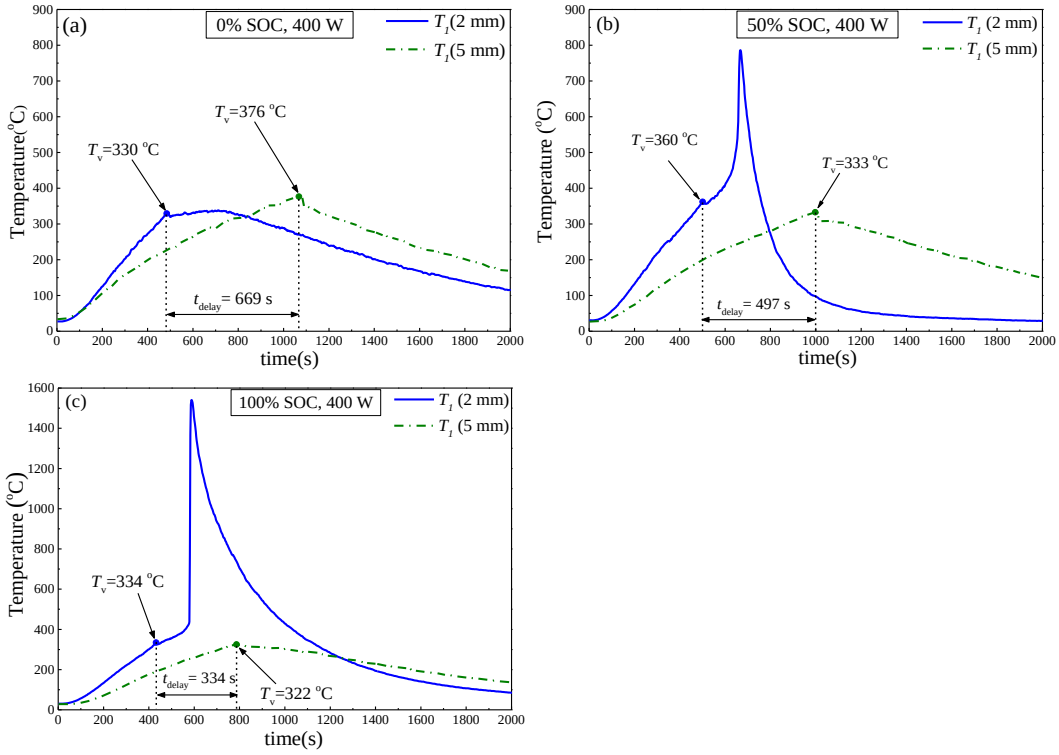

Fig. 11. The temperature response for the tests with different SOCs that the cell are heated by 400 W heater at 2 mm and 5mm spacing, respectively.

The values of transferred heat from heater to LIB through conduction and radiation in Tests 11-16 are shown in Fig. 12. The result indicates that the total transferred heat was approximately 9.94-13.73 kJ in Tests 11-13 with 2 mm spacing. When the spacing was increased to 5 mm in Tests 14-16, the transferred heat was approximately 20.52-30.12 kJ due to the improved heat dissipation condition and the delayed venting time. Besides, it can be seen that the radiation was the dominated way to trigger the safety venting of LIB as the large temperature difference between the surfaces of heater and LIB. The heat transferred by radiation accounts for 72.1%-73.6% in Tests 14-16 with 5 mm spacing, which was 56.1-61.0% for Tests 11-13 with 2 mm spacing.

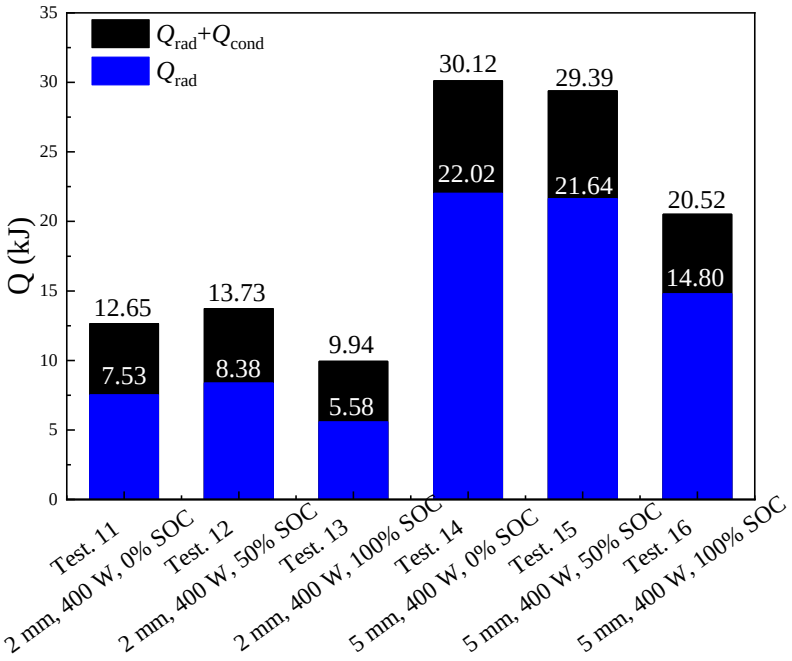

Fig. 12. The radiation and conduction heat in Tests 11-16 with with various SOCs (0%, 50%, 100%), and the cells are heated at 2 mm spacing in Tests 11-13 while 5 mm in Tests 14-16.

4. Conclusions

A series of experiments were carried out to investigate the impact of SOC, the power of the heater and cell spacing on thermal behavior of the lithium-ion battery on side-heating condition. The venting and maximum temperature of LIB in thermal runaway was measured as well the heat transfer path between heater and LIB was investigated. The primary conclusions are summarized as follows:

a) Thermal runaway behavior of lithium-ion battery was significantly alleviated with the decreasing SOC. In these experiments, the 50% SOC is an unstable state of the LIB that the ejected flame occurred frequently while the SOC of lithium-ion battery was higher than 50%. However, this jet flame phenomenon was totally replaced by a considerable amount of smoke when the SOC of LIB is less than 50%.

b) The maximum temperature of LIB in thermal runaway is linearly related to its SOC as more electric energy was stored in the LIB with higher SOC. However, the SOC shows slight effect on venting temperature as this behavior was determined by the reaction between the intercalated lithium and electrolyte solvents, that the venting temperature was approximately 136-165 ^{o}C in tests with 200 W heater.

c) The increased spacing and lower heating power both contribute to the preventing of thermal runaway behavior. The maximum temperature of the 200 W heater is around 700-800 ^{o}C, which is close to the peak temperature of the LIB in thermal runaway. And the result indicates that 2 mm spacing can significant prevent the thermal runaway propagation event between two LIBs system.

d) The amount of transferred heat between heater and LIB was calculated in this work. It indicates that the heat conduction through the air accounts for around 87.7-88.3% of the total transferred heat in tests with 2 mm spacing and 200 W heater. However, the radiation heat was the dominated way to transfer heat in tests with 400 W heater as the significant temperature difference between the heater and the LIB, that around 56.1-61.0% in tests with 400 W heater and 2 mm spacing while approximately 72.1%-73.6% in tests with 400 W heater and 5 mm spacing.

This work investigates the nature of hazards for LIB in side-heating condition, which is similar to the thermal runaway propagation process between LIBs. The dominated heat transfer path between the two cylinders system including the heater and LIB was analyzed, and the results can provide valuable guidelines for safety design of lithium-ion battery modules. In addition, there are also some deficiencies in this work. The temperature variation of the heater is different from the LIB in thermal runaway although the shape and size of the heater are designed to be the same as 18650 LIB. The critical heat energy on the battery thermal runaway behavior of lithium-ion battery will be further investigated in our future work.

Acknowledgements

This work is supported by the National Natural Science Foundation of China (No. 51674228), and the Fundamental Research Funds for the Central Universities (No. WK2320000038). Dr. Q.S Wang is supported by Youth Innovation Promotion Association CAS (No.2013286).

References

Bergman, T. L., Incropera, F. P., DeWitt, D. P. & Lavine, A. S. (2011). Fundamentals of heat and mass transfer, John Wiley & Sons.

Biensan, P., Simon, B., Peres, J., De Guibert, A., Broussely, M., Bodet, J. & Perton, F. (1999). On safety of lithium-ion cells. Journal of Power Sources, 81: 906-912.

Feng, X., He, X., Ouyang, M., Lu, L., Wu, P., Kulp, C. & Prasser, S. (2015). Thermal runaway propagation model for designing a safer battery pack with 25ah linixcoymnzo2 large format lithium ion battery. Applied Energy, 154: 74-91.

Feng, X., Sun, J., Ouyang, M., Wang, F., He, X., Lu, L. & Peng, H. (2015). Characterization of penetration induced thermal runaway propagation process within a large format lithium ion battery module. Journal of Power Sources, 275: 261-273.

Fu, Y., Lu, S., Li, K., Liu, C., Cheng, X. & Zhang, H. (2015). An experimental study on burning behaviors of 18650 lithium ion batteries using a cone calorimeter. Journal of Power Sources, 273: 216-222.

Jhu, C.-Y., Wang, Y.-W., Wen, C.-Y. & Shu, C.-M. (2012). Thermal runaway potential of licoo2 and li(ni1/3co1/3mn1/3)o2 batteries determined with adiabatic calorimetry methodology. Applied Energy, 100: 127-131.
Jhu, C. Y., Wang, Y. W., Shu, C. M., Chang, J. C. & Wu, H. C. (2011). Thermal explosion hazards on 18650 lithium ion batteries with a vsp2 adiabatic calorimeter. J Hazard Mater, 192(1): 99-107.
Kong, W., Li, H., Huang, X. & Chen, L. (2005). Gas evolution behaviors for several cathode materials in lithium-ion batteries. Journal of power sources, 142(1-2): 285-291.
Lamb, J., Orendorff, C. J., Steele, L. A. M. & Spangler, S. W. (2015). Failure propagation in multi-cell lithium ion batteries. Journal of Power Sources, 283: 517-523.
Larsson, F., Bertilsson, S., Furlani, M., Albinsson, I. & Mellander, B.-E. (2018). Gas explosions and thermal runaways during external heating abuse of commercial lithium-ion graphite-licoo2 cells at different levels of ageing. Journal of Power Sources, 373: 220-231.
Larsson, F. & Mellander, B.-E. (2014). Abuse by external heating, overcharge and short circuiting of commercial lithium-ion battery cells. Journal of The Electrochemical Society, 161(10): A1611-A1617.
Lisbona, D. & Snee, T. (2011). A review of hazards associated with primary lithium and lithium-ion batteries. Process Safety and Environmental Protection, 89(6): 434-442.
Liu, X., Stoliarov, S. I., Denlinger, M., Masias, A. & Snyder, K. (2015). Comprehensive calorimetry of the thermally-induced failure of a lithium ion battery. Journal of Power Sources, 280: 516-525.
Lopez, C. F., Jeevarajan, J. A. & Mukherjee, P. P. (2015). Characterization of lithium-ion battery thermal abuse behavior using experimental and computational analysis. Journal of The Electrochemical Society, 162(10): A2163-A2173.
Lopez, C. F., Jeevarajan, J. A. & Mukherjee, P. P. (2015). Experimental analysis of thermal runaway and propagation in lithium-ion battery modules. Journal of the Electrochemical Society, 162(9): A1905-A1915.
Nedjalkov, A., Meyer, J., Köhring, M., Doering, A., Angelmahr, M., Dahle, S., Sander, A., Fischer, A. & Schade, W. (2016). Toxic gas emissions from damaged lithium ion batteries—analysis and safety enhancement solution. Batteries, 2(1).
Peng, P., Sun, Y. & Jiang, F. (2014). Thermal analyses of licoo2 lithium-ion battery during oven tests. Heat and Mass Transfer, 50(10): 1405-1416.
Spotnitz, R. & Franklin, J. (2003). Abuse behavior of high-power, lithium-ion cells. Journal of Power Sources, 113(1): 81-100.
Sun, J., Li, J., Zhou, T., Yang, K., Wei, S., Tang, N., Dang, N., Li, H., Qiu, X. & Chen, L. (2016). Toxicity, a serious concern of thermal runaway from commercial li-ion battery. Nano Energy, 27: 313-319.
Wang, Q., Huang, P., Ping, P., Du, Y., Li, K. & Sun, J. (2017). Combustion behavior of lithium iron phosphate battery induced by external heat radiation. Journal of Loss Prevention in the Process Industries, 49: 961-969.
Wang, Q., Ping, P., Zhao, X., Chu, G., Sun, J. & Chen, C. (2012). Thermal runaway

caused fire and explosion of lithium ion battery. Journal of Power Sources, 208: 210-224.
Wang, Q., Sun, J., Yao, X. & Chen, C. (2006). Micro calorimeter study on the thermal stability of lithium-ion battery electrolytes. Journal of Loss Prevention in the Process Industries, 19(6): 561-569.
Wu, T., Chen, H., Wang, Q. & Sun, J. (2018). Comparison analysis on the thermal runaway of lithium-ion battery under two heating modes. J Hazard Mater, 344: 733-741.
Zhong, G., Li, H., Wang, C., Xu, K. & Wang, Q. (2018). Experimental analysis of thermal runaway propagation risk within 18650 lithium-ion battery modules. Journal of The Electrochemical Society, 165(9): A1925-A1934.

Table captions

Table 1 Experimental conditions of side-heating tests.

Table 2 Venting (T_v) and maximum temperature (T_{max}) of the LIB in Tests 1-7 with various SOCs.

Figure captions

Fig. 1. The arrangement of the devices and the location of thermocouples.

Fig. 2. Schematic of the experimental devices; a) photo of the battery safety control cabinet; b) photo of the K-type thermocouple; c) photo of the temperature logger module.

Fig. 3. The measured temperature and temperature rate responses for the LIB with 100% SOC in Test 7 without spacing.

Fig. 4. The temperature and temperature rise rate in Tests 1-6 with the 200 W heater and various SOCs.

Fig. 5. Fitting curve of the maximum and venting temperature during thermal runaway as a function of SOC.

Fig. 6. The development of thermal runaway behavior in Test 1, 4 and 7; (a) photos of thermal runaway development of LIB with 0% SOC in Test 1; (b) photos of the thermal runaway development of LIB with 50% SOC in Test 4; (c) photos of the thermal runaway development of LIB with 100% SOC in Test 7.

Fig. 7. The thermal runaway behaviors in Tests 1-7 with various SOCs.

Fig. 8. The temperature response for the tests with various SOCs that the LIB are heated at 2mm spacing by 200 W and 400 W heaters, respectively.

Fig. 9. The radiation and conduction heat in Tests 8-13 with with various SOCs (0%, 50%, 100%), and the cells are heated by 200 W heater in Tests 8-10 while 400 W heater in Tests 11-13.

Fig. 10. The temperature response for the tests with different SOCs that the cell are heated by 200 W heater at 0 mm and 2mm spacing, respectively.

Fig. 11. The temperature response for the tests with different SOCs that the cell are heated by 400 W heater at 2 mm and 5mm spacing, respectively.

Fig. 12. The radiation and conduction heat in Tests 11-16 with with various SOCs (0%, 50%, 100%), and the cells are heated at 2 mm spacing in Tests 11-13 while 5 mm in Tests 14-16.